Journal of Statistical Physics, Vol. 53, Nos. 1/2, 1988

The Stochastic Liouville Equation and Padé Approximants

A. J. Dammers,[1,2] Y. K. Levine,[1] and J. A. Tjon[3]

Received March 10, 1988

The applicability of Padé approximant techniques to solving the stochastic Liouville equation is discussed. The special case of an axially symmetric spin system undergoing isotropic Brownian motion is studied. Two types of expansions are explored which yield efficient algorithms for spectral simulations.

KEY WORDS: ESR spectral simulations; stochastic Liouville equation; Padé approximants; convergence behavior; roundoff errors.

1. INTRODUCTION

The technique of spin labeling has been widely used in various branches of physics to study the dynamical behavior of a molecule in a thermal environment such as in a liquid or liquid crystal structure.[1] Information about the rotational motion can be extracted from electron spin spectroscopy via comparison of the experimental spectra with numerical simulations of theoretical models.[2] In these models the molecule is assumed to undergo thermal fluctuations due to the presence of the liquid. These fluctuations are described in terms of random variables, giving rise to the stochastic Liouville equation (SLE).[3,4] In the past the use of the SLE to treat the interaction of the spin-labeled molecule with the liquid has been highly successful.[2] The actual solution of the SLE in general can be found by inverting large matrices.[3–7] This calls for fast and efficient algorithms, which enable spectral simulations to be carried out in practice.

[1] Department of Molecular Biophysics, University of Utrecht, The Netherlands.
[2] Present address: Centre for Submicron Technology, Delft University of Technology, The Netherlands.
[3] Institute for Theoretical Physics, University of Utrecht, The Netherlands.

0022-4715/88/1000-0109$06.00/0

822/53/1-2-8

Of the various methods used, the Lanczos algorithm[5,8] proved to be the most efficient. Two related approaches[9,10] have also been discussed in the literature. One, by Giordano *et. al.*,[9] is based on the application of memory function techniques and leads to a continued fraction solution of the SLE. The second approach, put forward by us,[10] proposed the application of Padé approximant (PA) techniques. In this paper we present a comprehensive discussion of this.

In the next section we briefly describe the SLE for the case of an axially symmetric molecule. The solution of the SLE is studied in Section 3 using the PAs on the moments of the spectrum. As a result the unsaturated ESR frequency spectrum can be determined in an efficient way. Section 4 deals with an alternative application of the PAs where the absorption is calculated for a fixed frequency. Although rather slow, it has the distinct advantage of a considerably faster convergence rate of the PAs. Moreover, it can also be used in the case of saturation such as occurring in ELDOR and saturation transfer ESR experiments.[1] In the last section some concluding remarks are made.

2. FORMULATION OF THE PROBLEM

Consider a spin system in an external static magnetic field $\mathbf{H}_0$ undergoing a tumbling motion due to the presence of a liquid. As a typical example, let us consider the case of an axially symmetric nitroxide system ($I=1$, $S=1/2$) characterized by a diagonal g and hyperfine tensor A. The principal axes of these two magnetic tensors coincide. Their orientation can be characterized by the Euler angles. For a particular Ω the spin Hamiltonian is given by[2]

$$\mathscr{H}(\Omega)=\frac{\beta_e}{\hbar}\mathbf{H}_0\cdot\mathsf{g}\cdot\mathbf{S}-\gamma_e\mathbf{I}\cdot\mathsf{A}\cdot\mathbf{S}-\gamma_n\mathbf{H}_0\cdot\mathbf{I} \tag{1}$$

The orientation Ω can be considered as a stochastic variable due to the interaction with the environment. Its time dependence is determined by a stationary Markov process, satisfying[1-4]

$$\partial P(\Omega, t)/\partial t = -\Gamma_\Omega P(\Omega, t) \tag{2}$$

where $P(\Omega, t)$ is the probability of finding the molecule with an orientation Ω. In view of Eqs. (1)–(2), the density matrix $\rho(\Omega, t)$ for the spin system satisfies the SLE[1-4,7]

$$\partial\rho(\Omega, t)/\partial t = -i\mathscr{L}\rho \tag{3}$$

where $\mathscr{L}$ is the stochastic Liouville operator. It is defined in the direct product space of the functions of the stochastic variables Ω and the space of the electron and nuclear spin operators. In terms of the spin Hamiltonian we have

$$\mathscr{L} = \mathscr{H}(\Omega)^X - i(\Gamma_\Omega + \Gamma_R) \tag{4}$$

where Γ_R is the spin relaxation operator describing relaxation processes other than the reorientational motion. We have here used the commutator superoperator notation $\mathscr{H}(\Omega)^X = [\mathscr{H}(\Omega),...]$. Using linear response theory, we can express the unsaturated ESR intensity of the absorption $\mathscr{A}$ as $\mathscr{A} = \mathrm{Im}\{I(z)\}$,[7] with

$$I(z) \propto \langle \Psi | \, [z - \mathscr{L}]^{-1} \, | \Psi \rangle \tag{5}$$

It is a function of the sweep variable $z = H_0 - \omega/|\gamma_e|$, with ω the microwave frequency and γ_e the electron gyromagnetic ratio. In Eq. (5), $|\Psi\rangle$ is the vector of the allowed spectral components. The molecule is assumed to undergo isotropic rotational Brownian motion characterized by a rotational diffusion constant D. For this case Γ_Ω is given by[2,12]

$$\Gamma_\Omega = -D\mathbf{L}^2/|\gamma_e| \tag{6}$$

where $\mathbf{L}$ is the angular momentum operator. It is now appropriate to choose in the Ω subspace the representation of Wigner rotational matrices $\mathscr{D}^L_{mn}(\Omega)$. Let the azimuthal quantum numbers of the electron and nuclear spin be given by β_k and ν_k, respectively. We may use as the basis set of states in the superspace

$$|L\nu_1\nu_2\gamma\rangle = \left(\frac{2L+1}{8\pi^2}\right)^{1/2} \mathscr{D}^L_{mn}(\Omega) \, |\beta_1\nu_1\rangle\langle\beta_2\nu_2| \tag{7}$$

to compute $I(z)$. Here, the symbol γ represents all the other quantum numbers m, n, β_1, and β_2. In the high H_0 field approximation, it is readily found using the axial symmetry that we have the selection rules for the operator $\mathscr{L}$

$$m = \nu_1 - \nu_2, \qquad L \text{ even}$$

while the electron spin quantum numbers are fixed, given by $\beta_1 = 1/2$ and $\beta_2 = -1/2$ and $n = 0$. In the representation (7), Γ_Ω is diagonal with elements

$$\langle L'\nu_1'\nu_2'\gamma' | \, \Gamma_\Omega \, | L\nu_1\nu_2\gamma\rangle = D\frac{L(L+1)}{|\gamma_e|}\delta_{LL'}\delta_{\nu_1\nu_1'}\delta_{\nu_2\nu_2'}\delta_{\gamma\gamma'} \tag{8}$$

The operator $\mathscr{L}$ reduces to an infinite matrix which has a banded structure, as shown schematically in Fig. 1. The nondiagonal elements arise from the matrix elements of the spin operators. For simplicity we assume that the spin relaxation operator Γ_R is diagonal in the nuclear spin space and that it can be characterized by a relaxation time T_2. In determining the ESR spectrum our major problem amounts to carrying out the matrix inversion needed in Eq. (5). This is done by truncating the matrix $\mathscr{L}$ at a sufficiently large value of $L = L_m$. The result of such a spectral simulation is shown in Fig. 2. A typical value of $L_m = 20$ is sufficient to reproduce the exact result of the infinite-dimensional case within an acceptable accuracy.

As the electronic gyromagnetic ratio γ_e is considerably larger than the nuclear one γ_n, we expect the nonsecular terms[12] in the spin Hamiltonian (1) to be effectively quenched.[1-6,12] Thus, no transitions within the nuclear spin system take place and for a given orientation Ω the spectrum will consist of three lines. However, the tumbling motion of the molecule modulates the spin Hamiltonian so that rather complex spectral shapes are observed as lines broaden substantially and superimpose. The detailed

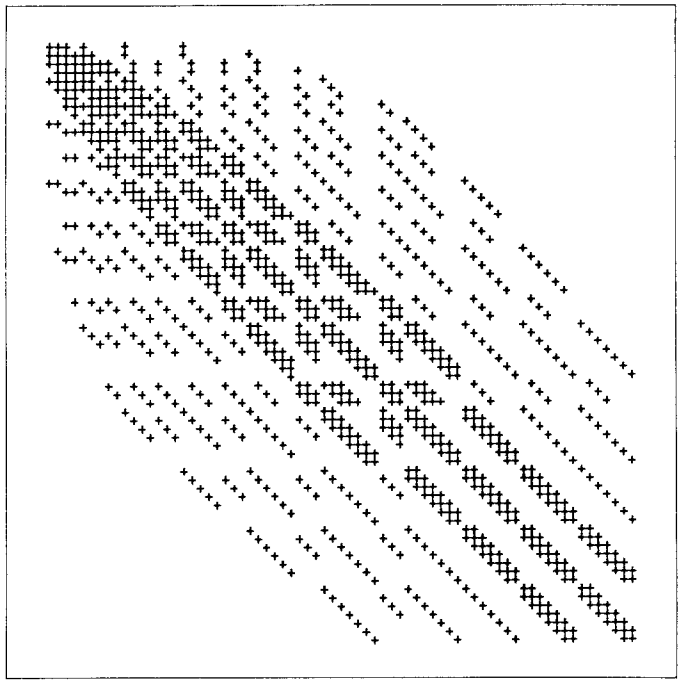

Fig. 1. Typical structure of the stochastic Liouville matrix. Each plus sign represents a nonzero element.

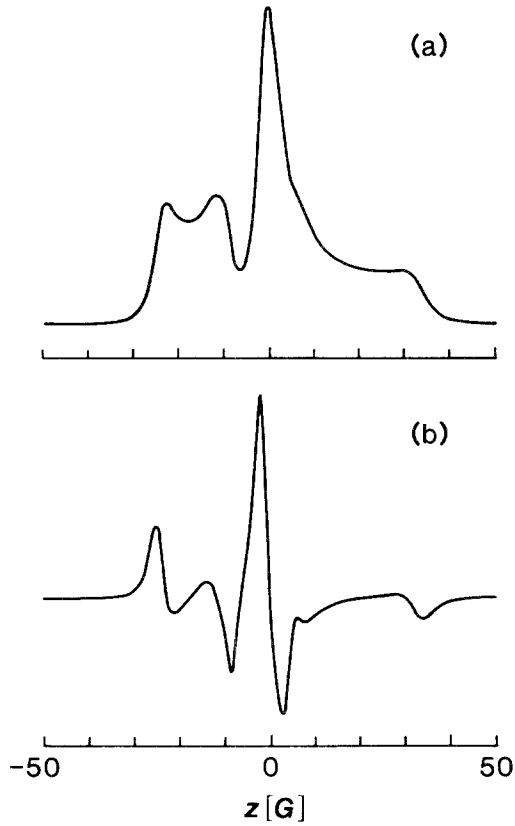

Fig. 2. (a) ESR absorption spectrum and (b) its first derivative of an axially symmetric ($I=1$, $S=1/2$) spin system as a function of the sweep variable $z=H_0-\omega/|\gamma_e|$. Parameters: $g_{\parallel}=2.0027$, $g_{\perp}=2.0075$, $A_{\parallel}=32$ G, $A_{\perp}=6$ G, $D=6.2\times10^{6}\,\mathrm{sec}^{-1}$, $T_2=2.18\times10^{-7}$ sec, $H_0=3200$ G.

spectral line shapes are in fact determined by the magnitude of the diffusion coefficient. Consequently, dynamical information can only be obtained from the experimental spectra from comparison with theoretical spectra simulated numerically. Since the numerical simulations have to be carried out many times, we need efficient methods to solve the Liouville equation. In the next section we discuss such a method.

3. ITERATIVE SOLUTION OF THE SLE

The construction of the solution to the SLE by straightforward matrix inversion is prohibitively time-consuming because of the large size of the

matrices involved. Consequently, attempts have been made to use iterative schemes. The SLE has the formal form

$$R\,|\Phi\rangle = |\Psi\rangle \tag{9}$$

with $R = z - \mathscr{L}$ and where Φ has to be determined. For any given non-singular operator Q, we may rewrire Eq. (9) as

$$|\Phi\rangle = K\,|\Phi\rangle + |\Phi_0\rangle \tag{10}$$

where the kernel is defined as

$$K = 1 - Q^{-1}R \tag{11}$$

and

$$|\Phi_0\rangle = Q^{-1}\,|\Psi\rangle \tag{12}$$

On introducing the complex multiplicative parameter κ into the kernel and carrying out the iteration implicit in Eq. (10), we find the Neumann series solution of Eq. (9). This yields the absorption spectrum as

$$I(z) = \sum_{n=0}^{\infty} \kappa^n \langle \Psi |\, K^n\, |\Phi_0\rangle \tag{13}$$

However, as the series solution (13) may not converge for $\kappa = 1$, an analytic continuation in the variable is in general needed. In the case of a compact operator Q such as the case of a nonsingular matrix of finite dimension, the solution of Eq. (10) is meromorphic in the parameter κ. Hence, the Padé approximant method[10,13–15] should be especially suitable for carrying out this analytic continuation.

The Padé approximant $[M/N]$ to a power series expansion of a function $F(\kappa)$ is defined as

$$[M/N](\kappa) = P_M(\kappa)/Q_N(\kappa) \tag{14}$$

such that

$$F(\kappa) - [M/N](\kappa) = O(\kappa^{M+N+1}) \tag{15}$$

Here $P_M(\kappa)$ and $P_N(\kappa)$ are polynomials in κ defined as

$$\begin{aligned} P_M(\kappa) &= p_0 + p_1\kappa + \cdots p_M\kappa^M \\ Q_N(\kappa) &= 1 + q_1\kappa + \cdots q_N\kappa^N \end{aligned} \tag{16}$$

The coefficients $\{p\}$ and $\{q\}$ appearing in Eq. (16) are determined uniquely from Eq. (14) on collecting equal powers of κ.

Let D be the dimension of the matrix K. Then it can immediately be seen that the $[D-1/D]$ approximant corresponds to the exact solution of Eq. (10). The main virtue of the Padé method is now that in practice a considerably lower order of PA is required to reconstruct the solution of the set of linear equations. Since D^2 operations are needed to reconstruct the solution iteratively using Eq. (10), whereas D^3 operations are required if matrix inversion methods are used, we see that a substantial amount of time can be saved using the above iteration schemes.

4. THE 1/z EXPANSION

Let us choose for the matrix $Q=\mathscr{L}$ and $\kappa=1/z$. The series solution for the absorption spectrum is then given by

$$I(z)=z^{-1}\sum_{n=0}^{\infty}a_n z^{-n} \tag{17}$$

where $a_n=\langle\Psi|\,\mathscr{L}^n\,|\Psi\rangle$. The coefficient a_n is the nth moment of $I(z)$, since

$$a_n=\int_0^{\infty} z^n I(z)\,dz \tag{18}$$

Our choice of the matrix Q greatly facilitates the calculation since the coefficients are not dependent on the sweep variable z. As a result the whole absorption spectrum can be readily determined once these coefficients have been calculated. We see from Eq. (17) that the Padé approximated solution is given by

$$I^{(M,N)}(z)=z^{-1}[M/N](z^{-1}) \tag{19}$$

We note that formally $I^{(M,N)}(z)$ can be seen as the $[M+1/N](z^{-1})$ Padé approximant to $I(z)$.

The evaluation of the Padé approximants is carried out by the application of recursive algorithms rather than a straightforward solution of Eq. (15).[13-15] Two such algorithms, those due to Wynn and Baker, have been found by us to be particularly useful. The Wynn algorithm affords the calculation of $[M/N]$ for a fixed value of $\kappa[\equiv 1/z]$, while the Baker algorithm enables the explicit determination of the coefficients $\{p\}$ and $\{q\}$. The latter algorithm is advantageous in our case for three reasons. First, $\mathrm{Im}\{I^{(M,N)}(z)\}$ can now be computed over the entire spectral range by a simple evaluation of the polynomials $P_M(1/z)$ and $Q_N(1/z)$. Second, it affords a direct evaluation of the experimental first derivative ESR spectrum $d/dz[I(z)]$ in closed form. Third, the explicit knowledge of the

polynomials $P_M(1/z)$ and $Q_N(1/z)$ allows the study of the distribution of poles and zeros of the Padé approximants. An inherent problem in the evaluation of Eq. (17) is the presence of a singularity at $z=0$. However, as the experimental spectrum is determined by real values of z only, the difficulties can be overcome by introducing an imaginary origin shift $z \to z + i\varepsilon$ and $A \to A + i\varepsilon$ in all the equations above. The consequences of such a shift will be discussed below. We note, furthermore, that the singularity at $z=0$ is absent in the $[N-1/N]$ Padé approximant to $I(z)$ since

$$I^{(N-1,N)}(z) = \frac{p_0 z^{N-1} + p_1 z^{N-2} + \cdots p_{N-1}}{1 + q_1 z^{N-1} + \cdots q_N} \tag{20}$$

The above Padé sequence has been applied to determine the absorption spectrum shown in Fig. 2. A typical value of $N=20$ is needed to reach convergence. The differentiation of the absorption spectrum $I^{(M,N)}(z)$ can be carried out numerically using cubic spline or other techniques. However, we have found it more convenient to evaluate the experimental signal in closed form from the coefficients $\{p\}$ and $\{q\}$ obtained via the Baker algorithm. It can be shown from Eqs. (16) and (19) that

$$\frac{d}{dz} I^{(M,N)}(z) = z^{N-M-1} \left[\frac{1+M-N}{z} \frac{P_M}{Q_N} - \frac{Q_N P'_M - P_M Q'_N}{Q_N^2} \right] \tag{21}$$

where

$$\begin{aligned} P_M &= \sum_{n=0}^{M} p_n z^{M-n}, \qquad P'_M = \sum_{n=0}^{M-1} (M-n)\, p_n z^{M-n-1} \\ Q_N &= \sum_{n=0}^{N} q_n z^{N-n}, \qquad Q'_N = \sum_{n=0}^{N-1} (N-n)\, q_n z^{N-n-1} \end{aligned} \tag{22}$$

and $q_0 = 1$. When $M = N-1$, Eq. (21) simplifies to

$$\frac{d}{dz} I^{(N-1,N)}(z) = -\frac{Q_N P'_{N-1} - P_{N-1} Q'_N}{Q_N^2} \tag{23}$$

Equation (23) has in fact been used in the evaluation of the experimental signal shown in Fig. 2.

The function $I(z)$ can be approximated by a hierarchy of Padé approximants $[M/N]$. The question arises as to the most suitable or convenient choice for the implementation of the numerical calculations. We shall investigate this by considering the properties of $I^{(M,N)}(z)$ for $z \to 0$. This approximant has the explicit form

$$I^{(M,N)}(z) = z^{N-M-1} F^{(M,N)}(z) \tag{24}$$

and

$$F^{(M,N)}(z)=\frac{p_0 z^M + p_1 z^{M-1} + \cdots p_M}{z^N + q_1 z^{N-1} + \cdots q_N} \tag{25}$$

It can be seen from Eq. (24) that we can impose poles or zeros of any order at $z=0$ simply by varying the difference $(M-N)$. These poles/zeros, however, tend to be compensated by $F^{(M,N)}(z)$. This is illustrated by an analysis of the three approximants $[N-1/N+1]$, $[N-1/N]$, and $[N/N]$,

$$I^{(N-1,N+1)}(z)=zF^{(N-1,N+1)}(z) \tag{26a}$$

$$I^{(N-1,N)}(z)=F^{(N-1,N)}(z) \tag{26b}$$

$$I^{(N,N)}(z)=z^{-1}F^{(N,N)}(z) \tag{26c}$$

The locations of the poles and zeros close to the real axis of z of the functions $F^{(N-1,N+1)}(z)$, $F^{(N-1,N)}(z)$, and $F^{(N,N)}(z)$ are shown in Fig. 3 for

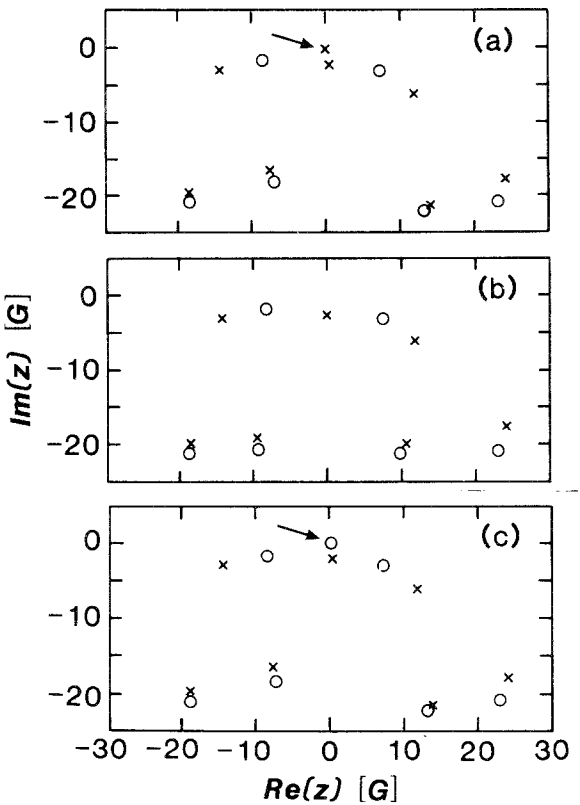

Fig. 3. Distribution of (×) poles and (0) zeros near the real z axis of (a) $F^{(24,26)}(z)$, (b) $F^{(24,25)}(z)$, and (c) $F^{(25,25)}(z)$. The model parameters are as given in Fig. 2 except for $D=6.2\times10^7\ \mathrm{s}^{-1}$.

$N = 25$. The figure shows that $F^{(24,26)}(z)$ possesses a pole at $z \sim 0$, which approximately compensates the zero imposed on $I^{(24,26)}(z)$, Eq. (26a). Similarly, $F^{(25,25)}(z)$ possesses a zero at $z \sim 0$, which compensates the pole imposed on $I^{(25,25)}(z)$, Eq. (26c). In marked contrast, $F^{(24,25)}(z)$ possesses neither a pole nor a zero at $z = 0$. As the locations of other poles and zeros are virtually identical for all the three cases considered, we choose the $I^{(N-1,N)}(z)$ approximant for practical applications. It has also the proper asymptotic behavior for $z \to \infty$.

The occurrence of pole/zero pairs in $I^{(N-1,N)}(z)$, shown in Fig. 3, can be understood from the decomposition of the PA in partial fractions. On setting $\{\lambda_j\}$ as the poles of $I^{(N-1,N)}(z)$, we can write this approximant as

$$I^{(N-1,N)}(z) = \sum_{k=1}^{N} W_k/(z-\lambda_k) \tag{27}$$

Here the weight factor W_k is the residue of $I^{(N-1,N)}(z)$ at $z = \lambda_k$,

$$W_k = p_0 \prod_{i=1}^{N-1} (z_i - \lambda_k) \Big/ \prod_{i=1}^{N}{}' (\lambda_i - \lambda_k) \tag{28}$$

where $\{z_i\}$ are the zeros of $I^{(N-1,N)}(z)$ and the prime indicates that $i = k$ is excluded from the product in the denominator. It can be seen from Eq. (28) that the proximity of a zero z_i to a pole λ_k corresponds to a low-weight contribution of the corresponding complex Lorentzian to the lineshape function (27).

The calculations of the ESR spectra are performed with a sweep variable $z = H_0 - \omega/|\gamma_e|$, implying an origin shift to the approximate center

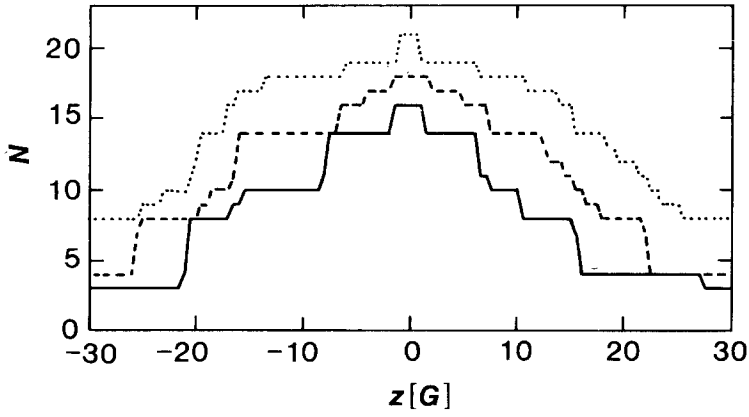

Fig. 4. Value of N required for $I^{(N-1,N)}(z)$ to reach convergence, as a function of the spectral position z (cf. Fig. 2). Criterion (see text): $\Delta \times 100\% =$ (—) 5%; (- -) 1%; (···) 0.1%. Parameters are as in Fig. 3.

of the spectrum at $\omega = |\gamma_e| H_0$. We shall now consider the convergence of the calculations for different parts of the spectrum, i.e., for different values of z, using the Wynn algorithm. The convergence behavior of $I^{(N-1,N)}(z)$ is shown in Fig. 4. Convergence is assumed if for two consecutive values of N the following condition is met:

$$\left| \frac{\mathrm{Im}\{I^{(N,N+1)}(z) - I^{(N-1,N)}(z)\}}{\mathrm{Im}\{I^{(24,25)}(0)\}} \right| < \Delta \tag{29}$$

Interestingly, we find that convergence occurs most slowly in the region $z \sim 0$. As power series in $1/z$ are involved in the construction of Padé approximants to $I(z)$, it is now interesting to consider whether an origin shift from $z = 0$ to $z = -\delta$ might influence the convergence. With this shift Eq. (17) now reads

$$I(z) = (z+\delta)^{-1} \sum_{n=0}^{\infty} a_n(\delta)(z+\delta)^{-n} \tag{30}$$

with $a_n(\delta) = \langle \Psi | (A+\delta)^n | \Psi \rangle$. However, it is known that the diagonal $[N/N]$ Padé approximants are invariant to the bilinear transformations which change Eq. (17) to Eq. (30).[13] Consequently, $I^{(N-1,N)}(z)$, which is formally the $[N/N]$ approximant to $I(z)$, is invariant under the origin shift and no acceleration of convergence can be obtained. This conclusion, however, does not hold for the other approximants $I^{(M,N)}(z)$ with $M \neq N-1$.

The result presented here shows that $I^{(N-1,N)}(z)$ is also invariant to the transformation $z \to z + i\varepsilon$ considered above as a means of avoiding singularities. However, it provides a justification for including a Lorentzian linewidth $\sigma_L = (|\gamma_e| T_2)^{-1}$ in the calculations through the simple substitution $z \to z + i\sigma_L$ in $I^{(N-1,N)}(z)$. This can be readily understood from the fact that this intrinsic lineshape enters the matrix $\mathscr{L}$, Eq. (5), as a scalar quantity $-i\sigma_L$, so that we have from Eq. (17)

$$I(z) = (z + i\sigma_L)^{-1} \sum_{n=0}^{\infty} a_n(0)(z+i\sigma_L)^{-n} \tag{31}$$

where the moments $a_n(0)$ are those obtained from the lineshape calculation with $\sigma_L = 0$.

We close this section by noting that the convergence of the Padé sequence may depend on the type of matrix elements studied. Let the nuclear spin degrees of freedom of the state $|\Psi\rangle$ be characterized by the quantum numbers v_j. The moment expansion, Eq. (17) of $I(z)$, can be expressed as

$$I(z) = 1/z \sum_n \sum_j a_n(j)(1/z)^n \tag{32}$$

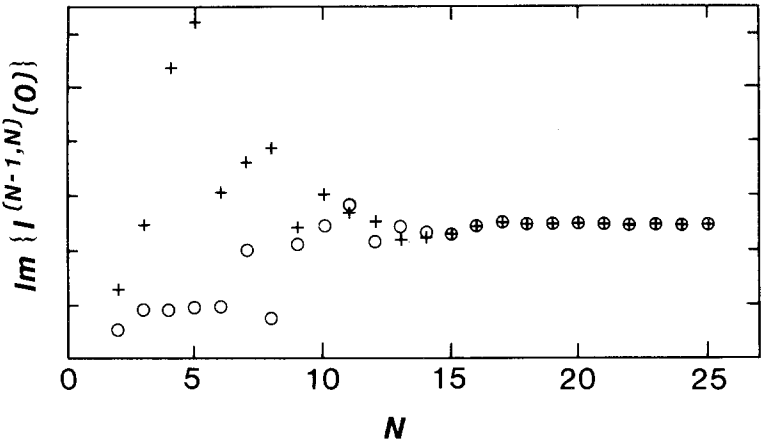

Fig. 5. Effect of summing the vector components prior to the calculation of $\mathrm{Im}\{I^{(N-1,N)}(0)\}$ (global approach), compared to a separate treatment. (0) Global approach; (+) separate; units of y axis are arbitrary. Parameters are as given in Fig. 3.

where

$$a_n^{(j)} = \langle \Psi | v_j \rangle \langle v_j | \mathscr{L}^n | \Psi \rangle \tag{33}$$

The evaluation of Eq. (32) can be carried out in two ways. The first is the global approach in which the summation over the index j is performed prior to the construction of the Padé approximant. Alternatively, the order of summation is interchanged and a Padé approximant is obtained separately for each value of j. However, it turns out that in calculations of ESR spectra in the slow motion regime the difference between the two approaches is marginal, as shown in Fig. 5. It can be seen that the main difference arises only in the way the convergence is achieved.

5. APPROXIMANTS AT A FIXED SWEEP VARIABLE

The rate of convergence of the sequence of Padé approximants depends on the specific choice of the matrix Q, Eqs. (11), (12). In practice, Q should be chosen such that it resembles R to a certain extent, while on the other hand the computation of Q^{-1} should be substantially easier than that of R^{-1}. In this section we will explore a procedure which in principle can also be used for the case of saturation.[1,11,16] In that case the sweep variable z enters in a more complicated way as in Eq. (5), so that the dependence in z cannot be separated out in an explicit way.

Given the considerations above, it is natural to take as an alternative choice $Q = z - \mathscr{L}_D$, where $\mathscr{L}_D$ is the diagonal part of the Liouville operator

in the representation (3). Also in this case we may perform a shift δ in the variable z. The series solution then becomes

$$(z-\mathscr{L})^{-1}=(z+\delta-\mathscr{L}_D)^{-1} \times \sum_{n=0}^{\infty}(z+\delta-\mathscr{L}_D)^{-1}(\delta-\mathscr{L}-\mathscr{L}_D)^n \tag{34}$$

We have compared the rate of convergence of the PAs based on Eq. (34) with the PAs on the $1/z$ expansion. Since in calculating high-order PAs roundoff errors may lead to unreliable results, it is clear that any gain we obtain in the rate of convergence of the Padé sequence by the appropriate choice of the operator Q is important. The relative deviation Δ_N of the $[N-1/N]$ PA as a function of N using the $1/z$ expansion is shown in Fig. 6. It is defined as

$$\Delta_N=\left|\frac{\mathrm{Im}(I^{(N-1,N)}-I_{\mathrm{exact}})}{\mathrm{Im}(I_{\mathrm{exact}})}\right| \tag{35}$$

The sweep variable z has been taken to be zero, while the angular momentum has been truncated at $L_m=20$ and $L_m=30$. The I_{exact} was obtained by

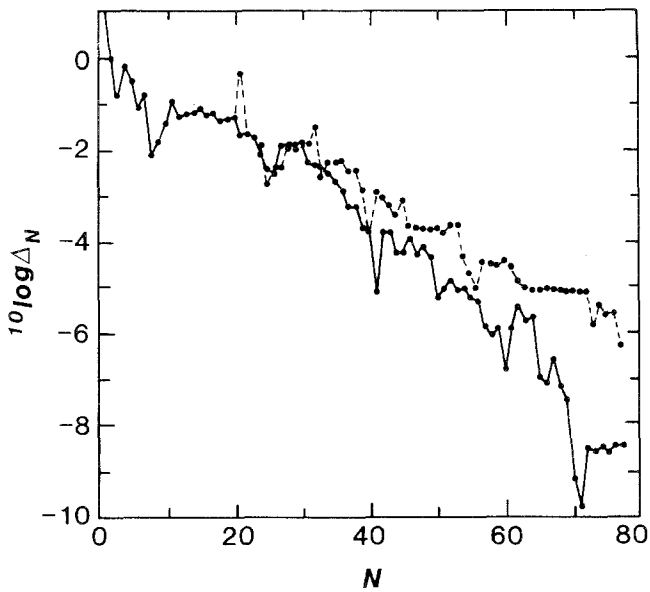

Fig. 6. Dependence of the relative deviation of the $[N-1/N]$ approximant on N, using the $1/z$ expansion for (—) $L_m=20$ and (- -) $L_m=30$. Parameters as given in Fig. 2.

exact diagonalization of $\mathscr{L}$, where $L_m = 30$ was used. A striking feature is the fact that the calculation with $L_m = 30$ converges more slowly than that with $L_m = 20$, but both give satisfactory results. Thus, increasing L_m from 20 to 30 yields no improvement of the final result, but it does slow down the convergence. The results of similar calculations, but now employing Eq. (34), are given in Fig. 7. The behavior of Δ_N for $L_m = 30$ is virtually indistinguishable from that for $L_m = 20$. Furthermore, convergence is considerably faster than found for the case of the $1/z$ expansion.

The slower convergence of the Padé sequence with increasing L_m in the case of the $1/z$ expansion can be understood by considering the eigenvalues λ_j of the kernel of Eq. (10). These eigenvalues lead to singularities in the absorption function $\mathscr{A}$. For increasing values of L_m, more eigenvalues appear, whose increasing imaginary parts are determined by the operator Γ_Ω. To a good approximation they are given by $\lambda_j \sim -iL(L+1)\,D/|\gamma_e|$. Although the contribution to $I(z)$ from the eigenstates with large λ_j can

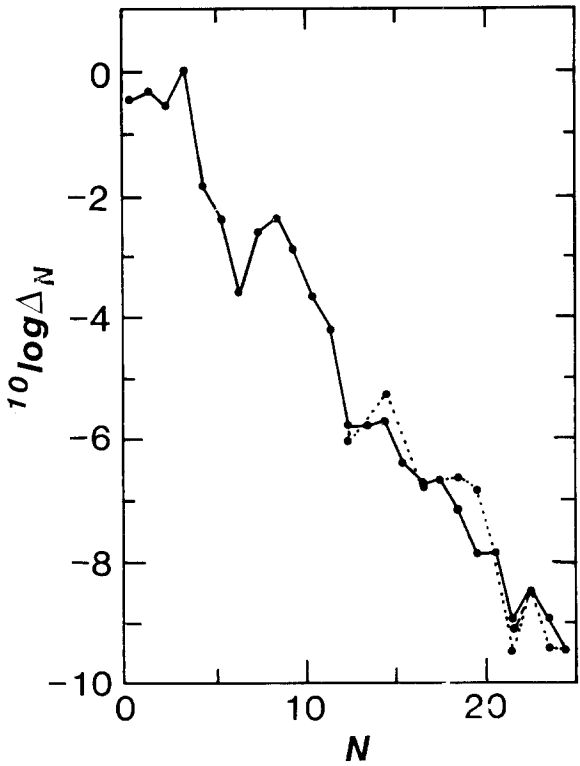

Fig. 7. The same as Fig. 6, but now based on the expansion (34) with $\delta = 10i$ G for (···) $L_m = 16$, (—) $L_m = 20$, and (- -) $L_m = 30$. The results for $L_m = 20$ and 30 coincide except for a small region near $N = 20$. Parameters as given in Fig. 2.

safely be neglected, the Padé sequence tends to include these eigenvalues as poles with appropriate weight. As a result, the singularities near the real z axis are represented less reliably, so that higher order approximants are needed to reach convergence. In marked contrast, these large eigenvalues are not present on taking $Q = z - \mathscr{L}_D$, so that only a limited range of eigenvalues λ_j need to be represented by the PA. Consequently, we do not now expect the convergence rate of the Padé sequence to detoriate with increasing L_m, as is indeed borne out in the actual calculations.

The approach discussed in this section suffers from the drawback that the iterative process must be repeated for every field point in the experimental spectrum. Thus, it will not provide as efficient an algorithm as that discussed in Section 4 and in ref. 5 using the Lanczos method. Nevertheless, we note that a similar formulation of the problem was adopted by Vasavada *et al.*[17] in their modification of the Lanczos algorithm. The importance of this method, however, is to be found in future applications to the numerical simulations of ESR experiments in the presence of a saturating microwave field, where no efficient algorithms currently exist.

5. CONCLUSIONS

We have here presented the main ingredients relevant for the application of the Padé approximation technique to the calculation of ESR spectra. We have shown on the basis of model calculations that the technique overcomes the problems of divergence inherent in moment expansion methods and provides a viable and efficient algorithm for the simulation of ESR spectra in the slow motion regime. We have further demonstrated that the Padé approximant $I^{(N-1,N)}(z)$ produces a reliable approximation to $I(z)$, the lineshape function. Importantly, this appoximant is convenient to implement in practical computations. It has further the remarkable property that it is invariant to the change of variable $z \to z + \delta$. This provides a simple way of including a homogeneous linewidth in the calculations.

An iterative scheme applicable to nonlinear ESR has been shown to give interesting results when applied to linear ESR. At the cost of having to perform the complete calculation for each value of the sweep variable separately, convergence was found to be improved considerably, so that it compares favorably to the Lanczos method. This faster convergence can be ascribed to the removal of the singularities arising from the Markovian operator Γ_Ω. In particular, for the case of simulations of the stochastic Liouville equation for saturation-type experiments the Padé technique should be a powerful tool.

REFERENCES

1. L. J. Berliner (ed.), *Spin Labeling* (Academic Press, New York).
2. J. H. Freed, in *Spin Labeling*, L. J. Berliner, ed. (Academic Press, New York), Chapter III.
3. J. H. Freed, in *Electron Spin Relaxation in Liquids*, L. T. Muus and P. W. Atkins, eds. (Plenum Press, New York, 1972), Chapter XIV.
4. R. G. Gordon and T. Messenger, in *Electron Spin Relaxation in Liquids*, L. T. Muus and P. W. Atkins, eds. (Plenum Press, New York, 1972), Chapter XIII.
5. G. Moro and J. H. Freed, *J. Chem. Phys.* **74**:3757 (1981).
6. J. H. Freed, in *Electron Spin Relaxation in Liquids*, L. T. Muus and P. W. Atkins, eds. (Plenum Press, New York, 1972), Chapter VIII.
7. E. Meirovitch *et al.*, *J. Chem. Phys.* **77**:3915 (1982).
8. C. Lanczos, *J. Res. Nat. Bur. Std.* **45**:255 (1950).
9. M. Giordano, P. Grigolini, D. Leporini, and P. Marin, *Phys. Rev. A* **28**:2474 (1983).
10. A. J. Dammers, Y. K. Levine, and J. A. Tjon, *Chem. Phys. Lett.* **88**:198 (1982), *J. Chem. Phys.* (1988) (in press).
11. H. Mori, *Progr. Theor. Phys.* **34**:399 (1965).
12. A. Abragam, *The Principles of Nuclear Magnetism* (Oxford University Press, London, 1961).
13. G. A. Baker, Jr., *Essentials of Padé Approximants* (Academic Press, New York, 1975).
14. P. R. Graves-Morris (ed.), *Padé Approximants* (Institute of Physics, London, 1973).
15. G. A. Baker, Jr., and J. L. Gammel (eds.), *The Padé Approximant in Theoretical Physics* (Academic Press, New York, 1970).
16. M. M. Dorio and J. H. Freed (eds.) *Multiple Electron Resonance Spectroscopy* (Plenum Press, New York, 1979).
17. K. V. Vasavada *et al.*, *J. Chem. Phys.* **86**:647 (1987).